



Open
Access

Simulation of Ammonia Looping Dissociation and Formation for Energy Conversion

Rizwan Ahmed Qamar¹, Asim Mushtaq^{2,*}, Ahmed Ullah¹, Zaeem Uddin Ali¹

¹ Chemical Engineering Department, NED University of Engineering & Technology, Karachi, Sindh, Pakistan

² Polymer and Petrochemical Engineering Department, NED University of Engineering & Technology, Karachi, Sindh, Pakistan

ARTICLE INFO

ABSTRACT

Article history:

Received 11 April 2020

Received in revised form 16 May 2020

Accepted 17 May 2020

Available online 15 August 2020

Production of energy by sustainable sources is increasing the significant attention of researchers because of cognizance of decreasing air pollution, emissions of carbon dioxide and less reliance on fossil-based powers. Numerous research works have been carried out in improving the efficiency of thermal storage plants technology, and different processes employing different methodologies are being utilized. The thirst for never-ending experiments has to lead the world towards ammonia-based working fluid as thermal storage based technology because of its high energy density and storage capacity. The thermal solar power plant studies with gaseous NH_3 as an operational liquid for the creation of energy in a Rankine cycle. This study aims to develop an effective storage system with thermochemical energy that stores, separates and synthesizes NH_3 to acquire power output. Thus, for this reason, plant simulation is accomplished on ASPEN PLUS, various models were enhanced through multiple factors and segments to get the most extreme power yield.

Keywords:

Ammonia; ASPEN; energy conversion;
Rankine cycle; thermal solar power plant

Copyright © 2020 PENERBIT AKADEMIABARU - All rights reserved

1. Introduction

In the coming a very long time of the destruction of the earth's fossil vitality shares, a power generation mix will assemble, which will be subject progressively by exchange and sustainable power sources. The elective energies are open as wind energy, solar energy, geothermal, hydroelectric, wave and tidal power, and so on. Sunlight based vitality can be applied likewise as a direct photovoltaic (PV) source or as concentrated solar power. Sunlight based warm vitality is concentrated utilizing various methods, for example, Parabolic Trough, power tower and dish system and so on. This study centers on using ammonia for vitality preservation by delivering power with the utilization of a solar plant from a sporadic vitality to a baseload power plant by including effective features for thermal storage. The accomplishment of solar thermal systems for power creation pivots

* Corresponding author.

E-mail address: engrasimmushtaq@yahoo.com

<https://doi.org/10.37934/arfmts.74.1.165188>

vitality on the selection, mechanical structure and optimal operation of a vitality storage system which can empower incessant operation of a power plant as appeared in Figure 1 [1, 2].

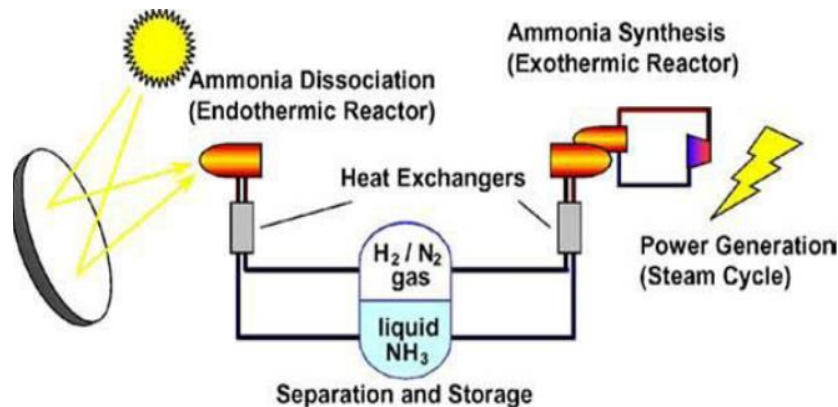


Fig. 1. The schematic diagram for power generation



Thermochemical energy storage for CSP is less established than liquid salt and other thermal storage strategies. However, it can accomplish advanced storage densities. Instead of storing heat by expanding the temperature of a substance or other CSP storage strategies, thermochemical capacity utilizes a reversible response to store vitality in synthetic securities. At the point when the reverse reaction is carried out, heat is discharged and utilized to run a thermal power cycle. The NH₃ thermochemical energy storage relies on the reversible separation of NH₃.



In this storage framework, a fixed stock of NH₃ passes consecutively among energy-storing (sunlight based separation) and vitality discharging (union) reactors, the two of which comprise a catalyst bed. Combined with a Rankine control cycle, the vitality discharging response could be utilized to create baseload power for the grid. This ultimate goal of this research is the utilization of NH₃ as a running fluid in thermal storage plant for power generation as an alternative to fuels to minimize CO₂ emission, store solar energy within the working fluid to utilize it in times of need. Parametric studies regarding optimized TSP design attained the aim of the research, numerical simulation of conservation equations, optimize physical dimensions of synthesis reactor, optimal distribution of catalyst (optimal control analysis) and overall thermal energy recovery analysis [3, 4].

Thermal energy from the sun is kept as chemical energy by a procedure named as solar thermochemical energy storage (TCES). Thermochemical storage has integrally higher vitality thickness than idle or reasonable heat storage plans because, sensible heat, vitality is stored as chemical potential. The endothermic responses that could be utilized for sunlight based TCES can work at fundamentally higher temperatures than current tech CSP storage frameworks. Worldwide CSP limit is still little contrasted with other sustainable power source innovations. However, it has been extending with a yearly development pace of about 40% since 2006. Advances in storage technologies could build a lot of the vitality portfolio is appeared in Figure 2 [5, 6].

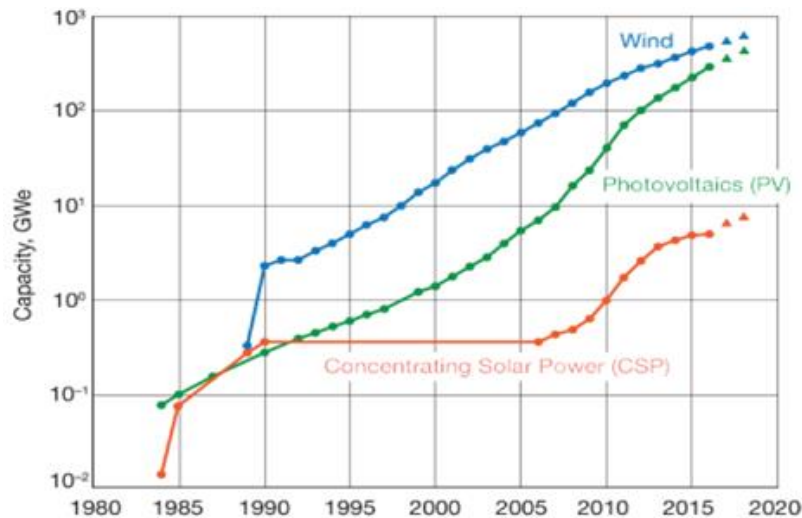


Fig. 2. CSP growth rate along the years

Fusing sunlight based TCES into CSP establishments requires a combination of an extra subsystem, a chemical plant for the reversible vitality storage responses. The subsystem gets heat from the solar collection field, which it can use to drive the endothermic vitality storage response when power isn't sought after. Since the reason for the chemical procedure is vitality storage, a basic segment of the subsystem is the storage tanks. Thermochemical storage instruments have a higher vitality density than thermal techniques, which could help lower capital expenses by decreasing storage tank volumes. At the point when vitality is required from storage, the TCES subsystem conveys heat to the power square is appeared in Figure 3. The reactants must get in touch with one another to respond, while heat is at the same time removed and sent to the power block. In a direct sun based TCES subsystem, the endothermic reactor gets heat straight from the solar receiver, while in an indirect subsystem. The endothermic reactor gets heat from the sunlight based assortment field using the heat-transfer fluid as display in Figure 4. The recipient and reactor are coupled in an immediate subsystem; heat-transfer fluid for extraordinary temperatures may not be accessible or down to earth for certain procedures [7, 8].

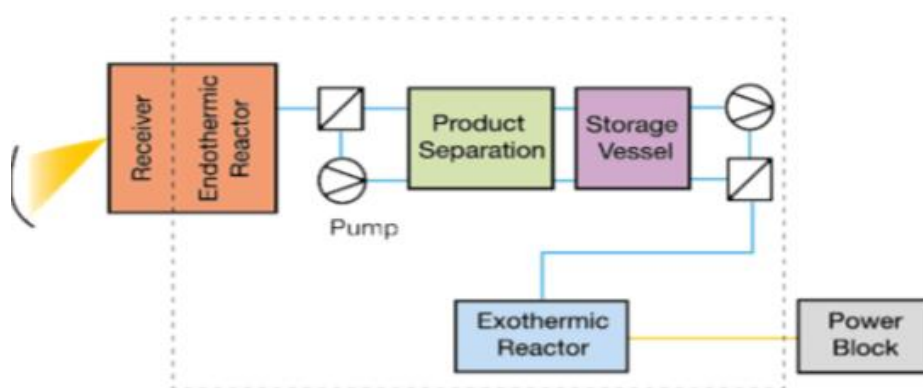


Fig. 3. Direct utilization of solar heat

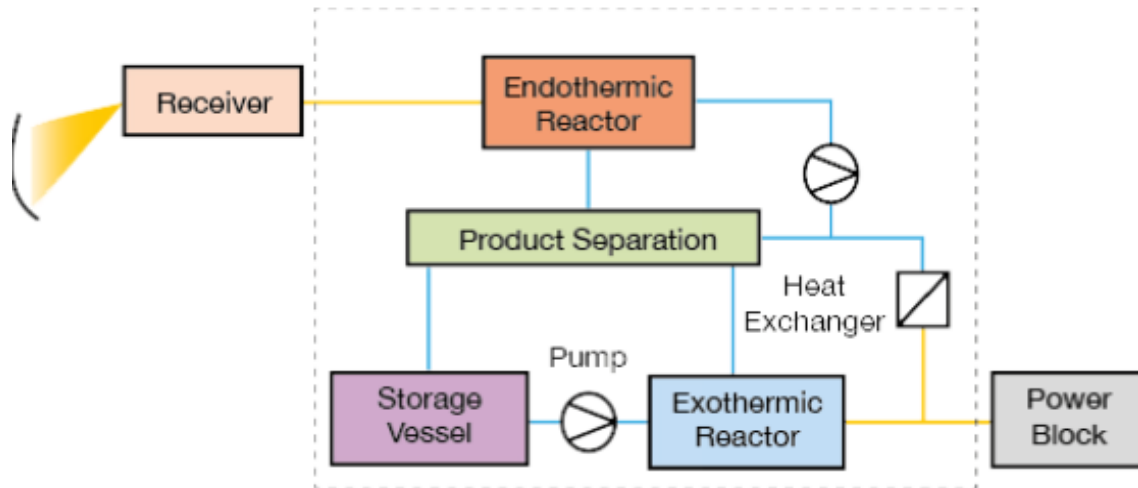


Fig. 4. Indirect utilization of solar heat

The utilization of fluid ammonia, as a thermo-substance energy storage medium, for endothermic separation by sun oriented vitality during insolation and resulting vitality recuperation by exothermic synthesis is viewed as a solid contender for the structure of a base-load solar thermal power plant. The innovation of NH_3 production is entrenched, similar to the simulation and modeling of ammonia synthesis. Although, optimization of the procedure is a continuing test as mechanical advancements empower better structures bringing about improved proficiency. As a major aspect of this optimization challenge, this study reflects the conceivable improvement in the recuperation of exothermic thermal vitality by optimization of the NH_3 synthesis process. While ammonia making has remained nearly the equivalent for a considerable length of time, the vitality utilization has diminished as innovation enhancements have been joined particularly for the manure business where over 90% of the vitality use is for ammonia synthesis. The raw materials and products are nitrogen (N_2), hydrogen (H_2) and ammonia (NH_3) [1, 6]. Table 1 shows the different studies regarding the ammonia-based storage system.

Table 1

Different studies regarding Ammonia-based storage system

Year	Ammonia-based storage system	Reference
Andreas Luzzi (1999)	Large paraboloid solar collectors and a thermochemical heat-pipe transport	[9]
K. Lovegrove (1999)	Solar-driven ammonia-based closed-loop	[10]
K. Lovegrove (2003)	Develop heat recovery reactors for manufacturing of superheated steam for Rankine cycle power systems works at a minimal power level of 1 kW	[11]
Mark A. Sutton (2008)	Highlighted volatilization sources of NH_3 .	[12]
Rebecca Dunn (2011)	Concentrating solar power (CSP) systems to create steam for instant electricity generation	[13]
H.L. Zhang (2013)	Give a method to predict hourly beam(direct) irradiation	[1]
M.E.E. Abashar (2016)	Simulates a cascade of multistage fixed bed membrane reactors to create great purity hydrogen appropriate for the PEM fuel cells	[14]
Trevor Brown (2017)	Turning an ammonia storage tank into a very large chemical battery.	[15]

Demand for electrical energy and the increasing needs for electrical and electronics system has become a part of modern society, and this need is increasing day by day. To fulfill this need, more fossil fuels are consumed and as a consequence, increased greenhouse gases like sulfur dioxide (SO₂), carbon dioxide (CO₂), nitrous oxide (NO_x) contaminates the environment to bring devastating effects on climate. Also, these finite resources of fossil fuels are rapidly depleting. Stemming for this problem there is a continuous search for new inexhaustible energy sources. Decrease of petroleum products at a fast rate and expanding of value makes essential the development of green power markets. As of now, there is a developing worldwide help for innovative work of sustainable power source advancements, especially for power generation [9-11,16-18].

2. Methodology

The system's thermal storage must be utilized to address the current gap amid the broken solar energy supply and the ceaseless power utilization. It includes three stages: storage, releasing and heat charging. The thermal energy storage innovations can be ordered by the system of heat through reasonable, inert, and chemical. In practical heat storage frameworks, through the charging step, sun oriented vitality is utilized to warm a liquid or a strong medium, in this way, increasing its vitality content. At this point, the medium is stored. When this vitality is discharged (releasing step), the temperature reduces. The sensible stored heat is related to this expansion or lessening of temperature. The thermal vitality kept by sensible heat storage can be evaluated as

$$Q = mC_p\Delta T \quad (3)$$

where; m = material mass (kg), C_p = specific heat over the temperature (kJ/kg.K) and ΔT = difference in temperature (K).

During the charging step in latent heat storage, sunlight based vitality can be utilized as the warmth source that starts a stage change. At the charging step, the medium is stored in its new stage. When this vitality is discharged, the second stage changes into the initial state. In the latent heat storage frameworks, organic compounds and inorganic compounds both can be utilized. The energy stored in the change stage can be computed as

$$Q = mL \quad (4)$$

where; m = material mass (kg) and L = latent heat of the material (kJ/kg). The thermochemical heat storage system consist of the following



In the endothermic response, heat is stored and discharged through exothermic one. The thermochemical heat stored is connected to the enthalpy reaction. Throughout the charging step, this vitality is utilized to separate a chemical reactant (A), results in (B and C); this is an endothermic reaction. In the discharging step, the results of the endothermic response (B and C) are combined and respond to shape the primary reactant (A), this response discharges heat and exothermic. The results of the two responses can be kept at surrounding or operating temperature. The vitality kept in a thermochemical medium can be stated as [2, 17]

$$Q = n_A\Delta H_r \quad (6)$$

where; n_A = number of mole of the reactant A (mol) and ΔH_r = enthalpy reaction (kWh/ mol A). The chemical reactions in a TES system are shown in Figure 5.

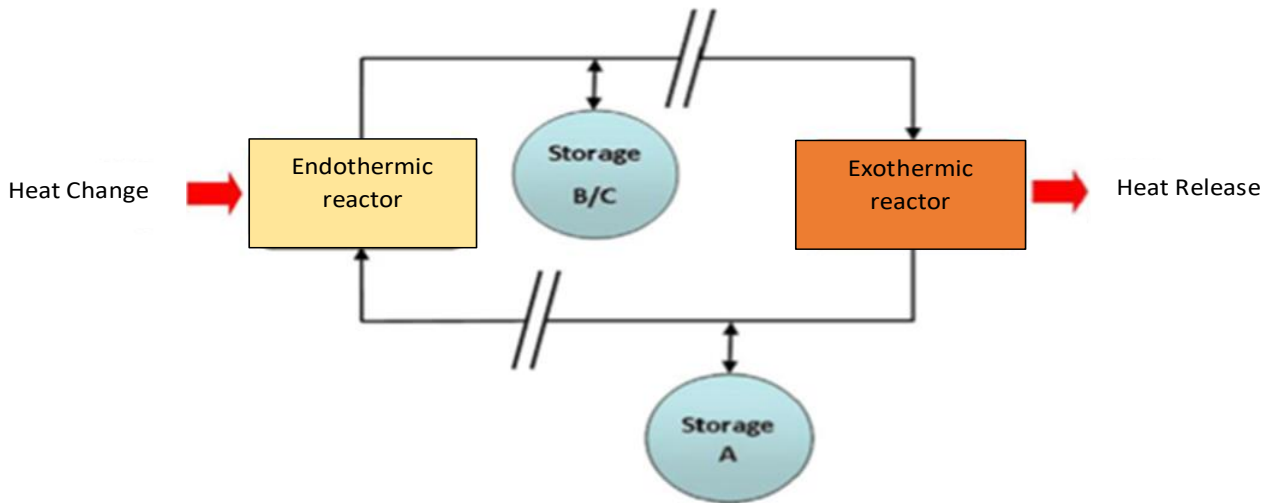


Fig. 5. Schematic of thermal energy storage (TES) system

There are two main kinds of solar energy systems use today: thermal systems and photovoltaics. Glass mirrors reflect ~92% of the daylight that hits them, are generally modest, can be cleaned, and keep going quite a while in the outside condition, settling on them a fantastic decision for the reflective surface of a sun powered concentrator. The dish structure must track the sun constantly to mirror the shaft into the thermal collector. Figure 6 shows the photovoltaic frameworks, convert sun oriented radiation to power using a range of techniques. The most widely known method is to utilize silicon boards that generate an electrical flow when light sparkles upon it [19, 20].



Fig. 6. Solar photovoltaic

2.1 Working Principles of Concentrating Collectors

In contrast to photovoltaic, which utilize light to generate power, concentrating sun oriented power frameworks produce power with heat. Concentrating solar collectors use mirrors and focal points to focus sunlight onto a heat collector, like a kettle tube. The collector retains and changes over daylight into heat. The heat is then conveyed to a steam generator or motor where it is changed over into power.

Trough frameworks prevail among the existing business solar power plants. Due to their parabolic shape, troughs can center the sun at 30 to multiple times its typical power on a collector pipe situated beside the central line of the trough. Manufactured oil catches this heat as the oil circles in the pipe, arriving at temperatures as high as 390°C (735°F). The hot oil is siphoned to a creating station and directed over a heat exchanger to deliver steam. At long last, power is delivered in a traditional steam turbine. Trough innovation is the economic sun oriented innovation accessible today [21, 22].

The power transformation unit incorporates the thermal receiver and the motor/generator. The thermal receiver is the interface between the dish and the motor/generator. It ingests the concentrated light emission vitality, changes over it to heat, and moves the heat to the motor/generator. A thermal receiver can be a bank of cylinders with a cooling liquid, normally helium or hydrogen, which is the heat move medium and the working liquid for a motor. Substitute thermal collectors are heat funnels wherein the bubbling and consolidating of a moderate liquid is utilized to move the heat to the motor. The motor/generator framework is the subsystem that takes the heat from the thermal collector and utilizes it to create power. The most widely recognized sort of heat engine utilized in dish-motor frameworks is the Sterling motor. A Sterling motor uses heat gave from an outside source (like the sun) to move cylinders and make mechanical power, utilized to drive a generator and produce electrical power.

Power towers ('heliostat' control plants) catch and center the sun's heat vitality with thousands of mirrors (called heliostats) in approximately a two square mile field. The heliostats center concentrated daylight around a receiver that sits over the tower. Inside the collector, the concentrated daylight heats liquid salt to more than 1,000 °F (538 °C). The heated molten salt at that point streams into a thermal storage tank where it is kept, 98% thermal productivity, and inevitably siphoned to a steam generator. The steam runs a turbine to create power. This procedure is recognized as the "Rankine cycle". The benefit of this structure over the parabolic trough design is the higher temperature. Thermal vitality at greater temperatures can be changed over to power all the more proficiently and is inexpensively stored for future use [23, 24].

2.2 Ammonia as a Working Fluid

NH₃ is a possibility for enormous solar-thermal schemes because of the capacity of thermal vitality in its chemical bonds in the sun based insolation and recuperation from exothermic production. To think about various storage systems, the vitality storage density is valuable to decide the needed capacity for a necessary measure of energy. With the sort of energy transporter, the measure of storage vitality changes emphatically. The ammonia-based framework has no bothersome side responses, the scope of standard catalysts, huge experience of industrial involvement in Haber Bosch process, utilization of gentle steel parts for taking care of and capacity, stage detachment of reactants and items at surrounding temperature, no issues with sun oriented drifters. Lower working temp for higher beneficiary effectiveness and fewer materials limitations, however high working weights, smallish enthalpy of response and transformation productivity restricted by low specific temperature. The different processes description for ammonia synthesis is given in Table 2 [25, 26].

Table 2
 Description of various processes for ammonia synthesis

Process	Year	Description
Haldor Topsoe Ammonia Synthesis Process	1999	improved catalysts strength, versatile, firm and poison-resistant catalyst, mostly magnetite Fe ₃ O ₄ with supporters mostly oxides of potassium, calcium and aluminum
Haldor Topsoe Ammonia Converter Features	1979	2 catalyst beds and 1 interbed heat exchanger
	1991	3 catalyst beds with 2 interbed heat exchangers
Kellog Brown & Roots (KBR) Advanced Ammonia Process (KAPP)	1992	Uses a high-pressure heat exchange relies on the steam reforming process integrated with a low-pressure. CO ₂ is removed from the process gas using methyl diethanolamine and hot potassium carbonate solution.
Krupp Uhde GmbH Ammonia Process	1994	The utilized reforming process followed by a medium-pressure NH ₃ synthesis loop.
ICI-Leading Concept Ammonia (LCA) Process	1992	NH ₃ synthesis takes place at low pressure with ICI's highly active cobalt promoted catalyst.
The Linde Ammonia Concept (LAC) Ammonia (LCA) Process	1998	The NH ₃ synthesis loop, based on Casale axial-radial 3 bed converter with internal heat exchanger giving a high conversion
The Haber Bosch Process	2001	This process combines nitrogen from the air with hydrogen derived mainly from natural gas into NH ₃

2.3 The Haber Bosch Process

The Haber process combines nitrogen from the air with hydrogen resulting from natural gas into NH₃ is shown in Figure 7. Ammonia (NH₃) stays in the liquid form at temperatures higher than its melting point -77.73 °C and has a density of 681.9 kg/m³ at its boiling point -33.34 °C ; it must thus be kept at very low temperature or stored at very high pressure. The production of NH₃ is exothermic, and the reaction is reversible.

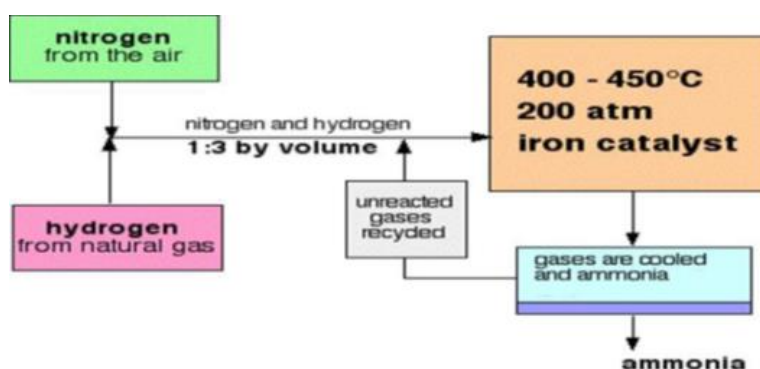
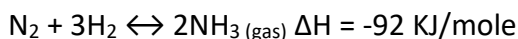


Fig. 7. Flow scheme of the Haber process

The catalyst is more complex; it has potassium hydroxide work as a supporter substance that builds its proficiency. The pressure differs from one developing plant then onto the next, however, it is in every case high. At each go of the gases through the reactor, just fifteen percent of the N and H₂ changes over to NH₃. By continuous reusing of the unreactive N and H₂, the over-all transformation is about 98%. It needs to change the position of the equilibrium on the distance to the right to create the extreme possible amount of NH₃ in the equilibrium mixture. As stated by Le Chatelier's Principle, if the pressure of the system increase, it will respond by supporting the reaction, which built fewer

molecules which will again reduce the pressure. You have to move the location of the equilibrium to one side to make the most extreme conceivable amount of NH_3 in the equilibrium mixture [27, 28].

Including a catalyst doesn't create any more percentage of NH_3 in the equilibrium mixture. It's the capacity to accelerate the reaction. The reaction is delayed without a catalyst to such an extent that no response occurs in any reasonable time. The catalyst ensures that the response is quick for a dynamic equilibrium. The gases are hot and at exceptionally high pressure when leaving the reactor. NH_3 is effectively liquefied under pressure.

2.4 Operational Parameters

The working conditions of TSP must be picked cautiously as the utilization of a reversible response to store vitality is represented by the reliance of the composition of thermodynamic equilibrium on pressure and temperature. The schematic outline of TSP has appeared in Figure 8. In this closed-loop framework, a fixed stock of NH_3 passes consecutively among vitality storing and vitality discharging reactors, the two of that comprise a catalyst bed. Combined with a Rankine control cycle, the vitality discharging response could be utilized to create baseload control for the grid.

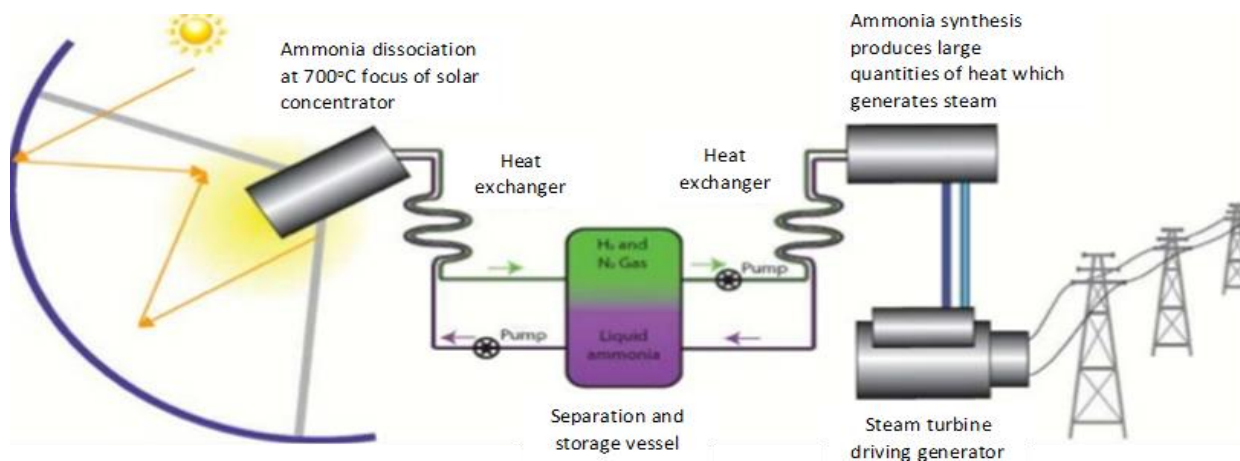


Fig. 8. Schematic diagram of the plant

Having the upside of sun oriented convergence of 3000 suns, a reflected paraboloid dish centers sun oriented radiation onto a separation reactor from which anhydrous NH_3 is siphoned. The reactor comprises an annular catalyst bed that encourages the separation of NH_3 at imperative pressure and temperature into vaporous nitrogen and hydrogen named "syngas". The way that the NH_3 separation response has no conceivable side responses produce sun-powered separation reactors simple to control and actualize. Commonly, 400 such reactors mounted on paraboloid dishes, of zone 400 m^2 each, are utilized in an exhibit designed to sustain the ammonia synthesis reactor [24, 29].

The Haber-Bosch process is the most conservative process for the obsession of nitrogen and with adjustments proceeds being used as one of the essential techniques of the chemical industry. The heat exchangers serve to move heat from leaving a response to the cool incoming water to change over into high-pressure steam. Likewise, the vehicle channeling and vitality storage volume are altogether worked at near ordinary temperature, diminishing thermal losses from the framework, just as taking out the requirement for specialized equipment. Compressors are utilized to keep up the pressure of 300 bar, while pumps are utilized to give vitality to water in the Rankine cycle. The thermochemical vitality storage utilizing NH_3 looping of the procedure has appeared in Figure 9.

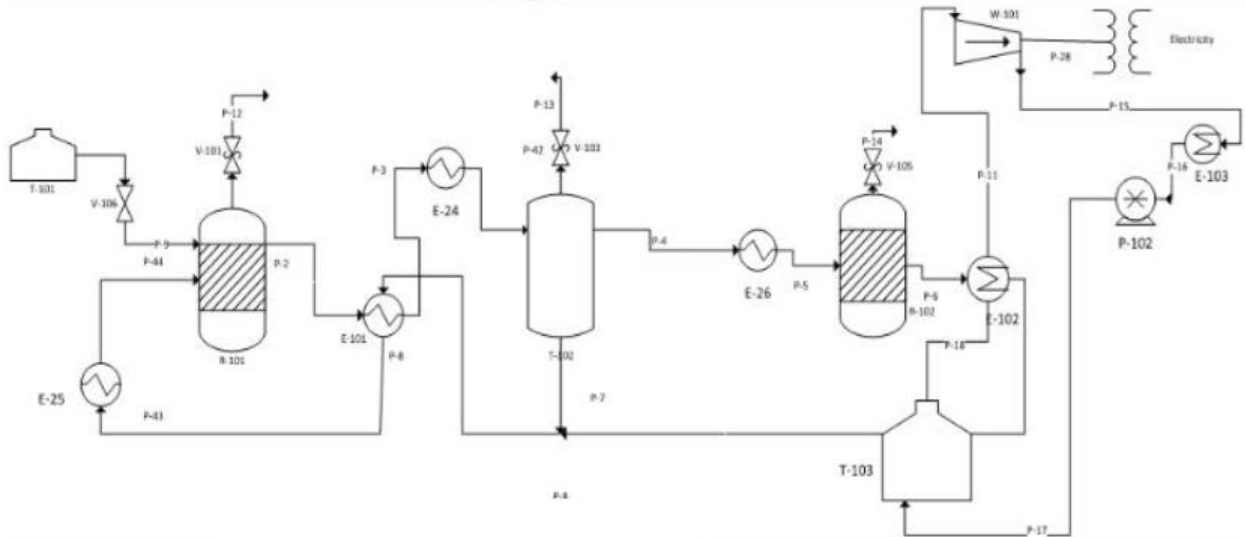


Fig. 9. Process flow diagram

3. Results

This simulation is done on ASPEN PLUS software. The numerous constituents used in plant modeling are given in Figure 10, and Figure 11 shows the fluid package used.

Components - Specifications

Selection Petroleum Nonconventional Enterprise Database Information

Select components

Component ID	Type	Component name	Alias
NH3	Conventional	AMMONIA	H3N
H2	Conventional	HYDROGEN	H2
N2	Conventional	NITROGEN	N2
WATER	Conventional	WATER	H2O

Find Elec Wizard User Defined Reorder Review

Fig. 10. Components used

Methods

Global Flowsheet Sections Referenced Information

Property methods & options

Method filter: COMMON
 Base method: NRTL
 Henry components: [dropdown]

Petroleum calculation options

Free-water method: STEAM-TA
 Water solubility: 3

Electrolyte calculation options

Chemistry ID: [dropdown]
 Use true components

Method name: NRTL

Modify

Vapor EOS: ESIG
 Data set: 1
 Liquid gamma: GMRENON
 Data set: 1
 Liquid molar enthalpy: HLMX85
 Liquid molar volume: VLMX01
 Heat of mixing
 Poynting correction
 Use liquid reference state enthalpy

Fig. 11. Fluid package used

In this study used PFR for the production and dissociation of NH_3 . The PFR (Plug Flow Reactor) for the most part comprises a set of cylindrical pipes or cylinders that have appeared in Figure 12. The stream field is demonstrated as an attachment stream, suggesting that the stream is radially isotropic. This additionally infers axial mixing is insignificant. Thus, the PFR, the reactor is isolated

into few subvolumes. Inside subvolume, the response rate and mole balance are viewed as spatially uniform [16, 30].

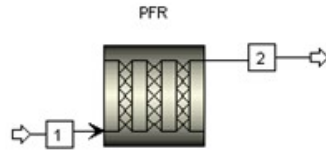


Fig. 12. PFR in ASPEN PLUS

The purpose of using the PFR reactor is as follows in Table 3.

Table 3

Comparison between PFR and FBR

In PFR	In FBR
Operates at 150 bar	Operates at 40 - 50 bar
The efficiency of 24-26%	The efficiency of 20%
Fe-Ni used as a catalyst	Ruthenium catalyst used

The dissociation reactor (simulation) reference has been used to evaluate equilibrium constant. The total Gibbs free energy of a mixture of reactants and products drives through a least value as the composition deviations then all net change will cease, the reaction system will be in a state of chemical equilibrium. You will recall that the relative concentrations of reactants and products in the equilibrium state is expressed by the *equilibrium constant*. Figure 13 shows the input parameters for the dissociator. Figure 14 explain the kinetic parameters for dissociator. Figure 15 the dissociation profile of reactants and products.

$$\log K = 2.6899 + 2001.6 \times T^{-1} + 1.8488663 \times 10^{-7} T - 2.691122 \log T - 5.519265 \times 10^{-5} T \quad (7)$$

where; T = absolute temperature in K.

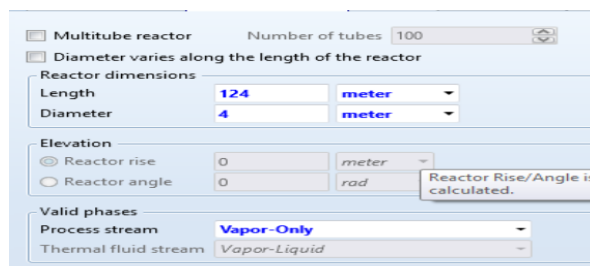


Fig. 13. Input parameters for dissociator

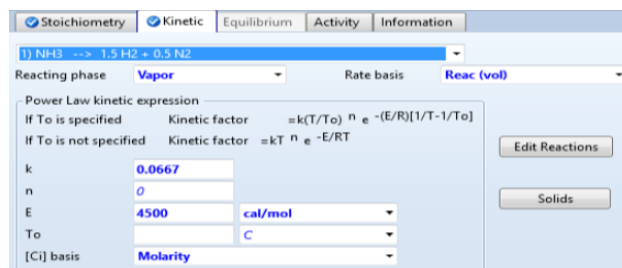


Fig. 14. Kinetic parameters for dissociator

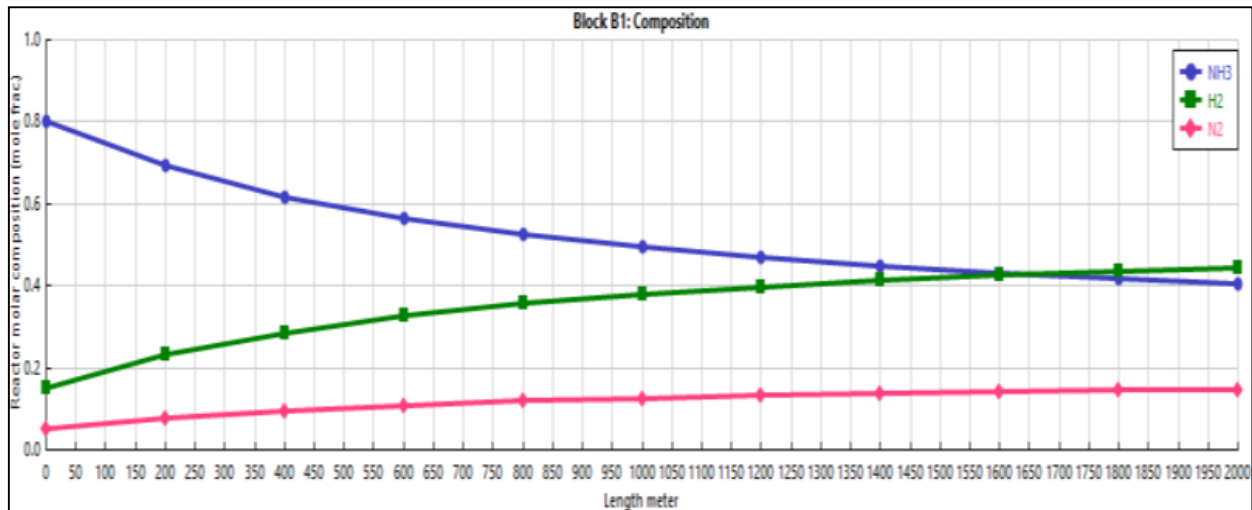


Fig. 15. Dissociation profile of reactant and products

The synthesis reactor (simulation) reference has been used to evaluate equilibrium constant. Figure 16 shows the input design parameters for the synthesis reactor. Figure 17 explains the kinetic factors for the synthesis reactor. Figure 18 the molar composition profile for the synthesis of ammonia [22, 31].

$$\log k = 2250.322T^{-1} - 0.85340 - 1.5049 \log T - 2.58987e^{-4T} + 1.48961e^{-7T^2} \quad (8)$$

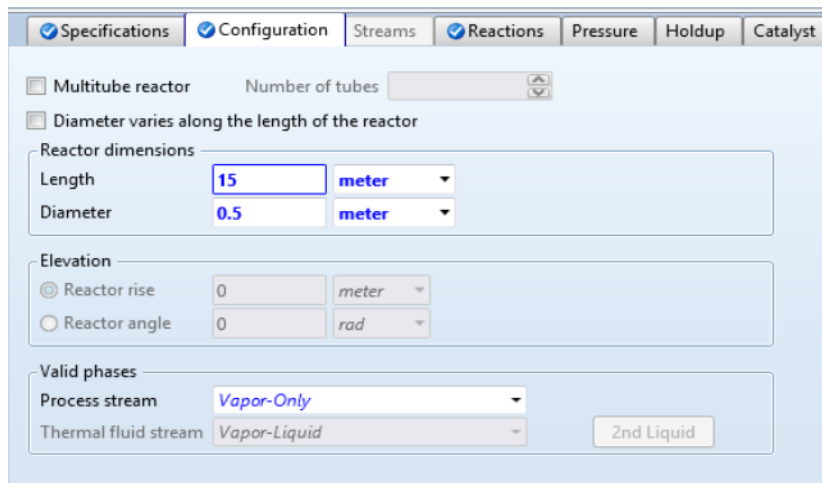


Fig. 16. Input design parameters for the synthesis reactor



Fig. 17. Kinetic factors for synthesis reactor

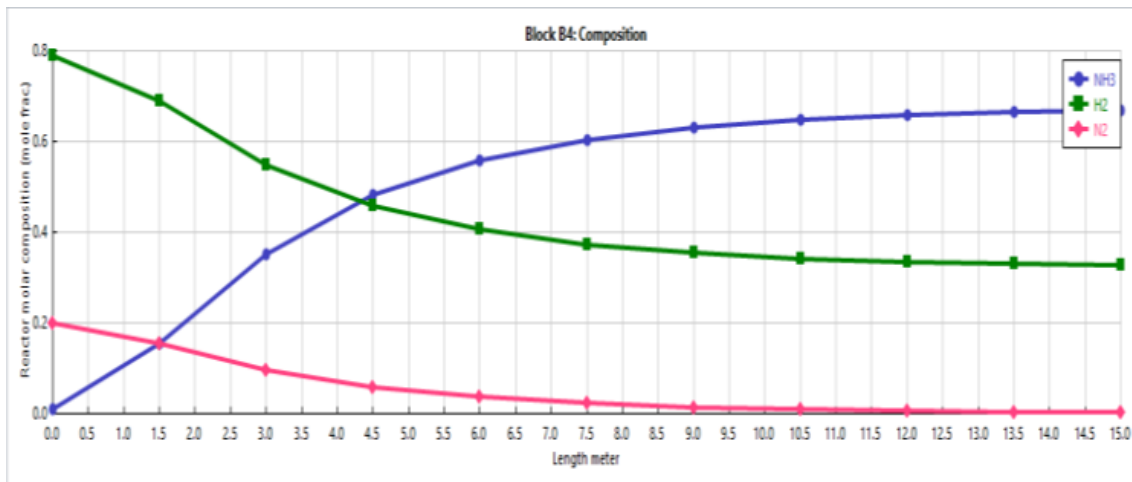


Fig. 18. Molar composition profile for the synthesis of ammonia

Here the purpose of the heater (source of csp) is to heat the working fluid that is ammonia to reach a temperature of 520°C which is sufficient temperature for the reaction to take place in deformer is shown in Figure 19 [32,33]. The input specification for the heater is shown in Figure 20.



Fig. 19. Heater

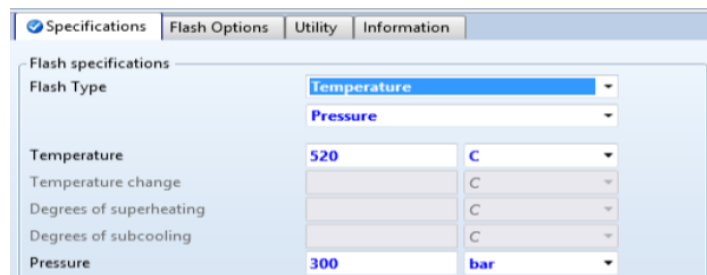


Fig. 20. Input specification for heater

The stream result worksheet for the heater is shown in Figure 21.

	Units	S7	S1
NH3	KMOL/HR	195.573	195.574
H2	KMOL/HR	102.987	102.985
N2	KMOL/HR	34.329	34.3285
WATER	KMOL/HR	0	0
Mole Flow	KMOL/HR	332.889	332.888
Mass Flow	KG/HR	4500	4500
Volume Flow	L/MIN	455.564	1219.58
Temperature	C	112.41	520
Pressure	BAR	300	300

Fig. 21. Worksheet for heater

Flash tank (separator), is used here to separate the vapor-liquid feed into separate vapor and liquid streams respectively using rigorous vapor-liquid equilibrium in Figure 22. The input specification for the flash tank shown in Figure 23. Stream result worksheet for flash tank explains in Figure 24.

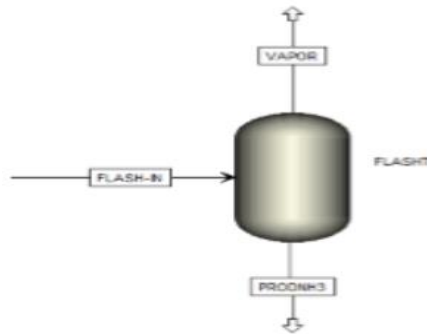


Fig. 22. Flash tank

Fig. 23. Input specification for flash tank

Default		Units	S2	S3	S4
NH3	KMOL/HR	3.8903	36.358	32.4677	
H2	KMOL/HR	341.236	341.809	0.573654	
N2	KMOL/HR	110.174	113.937	3.76267	
WATER	KMOL/HR	0	0	0	
Mole Flow	KMOL/HR	455.3	492.104	36.804	
Mass Flow	KG/HR	3840.5	4500	659.505	
Volume Flow	L/MIN	553.421	585.437	18.1141	
Temperature	C	-10	-4.0054	-10	
Pressure	BAR	300	300	300	

Fig. 24. Worksheet for flash tank

Figure 25 shows the mixer. Stream result worksheet for mixer shows in Figure 26.

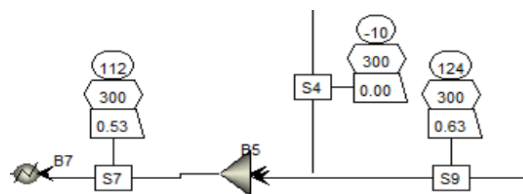


Fig. 25. Mixer

		Units	S4	S7	S9
Phase:			Liquid	Mixed	Mixed
Component Mole Flow					
NH3	KMOL/HR	32.4677	195.573	163.105	
H2	KMOL/HR	0.573654	102.987	102.413	
N2	KMOL/HR	3.76267	34.329	30.5663	
WATER	KMOL/HR	0	0	0	
Mole Flow	KMOL/HR	36.804	332.889	296.085	
Mass Flow	KG/HR	659.505	4500	3840.5	
Volume Flow	L/MIN	18.1141	455.564	459.824	

Fig. 26. Worksheet for Mixer

Figure 27 shows the heat exchanger. Heat exchanger result worksheet for mixer shows in Figure 28. The temperature achieved by exchanging heat in this exchanger is being used to generate high-pressure steam which is being used to generate power of about 2.5 MW is shown in Figure 29.

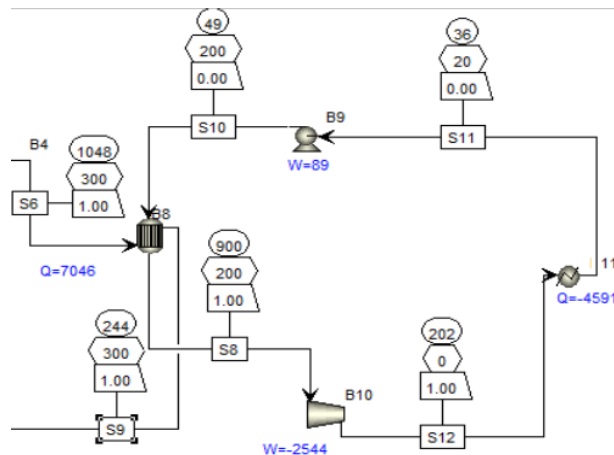


Fig. 27. Heat Exchanger

	S6	S10	S9	S8
Total Flow mol/sec	187.475	93.285	187.475	93.285
Total Flow kg/sec	2.34332	1.68056	2.34332	1.68056
Total Flow cum/sec	0.0686506	0.00173129	0.0268645	0.0454948
Temperature C	1048.14	48.7972	243.898	900
Pressure bar	300	200	300	200
Vapor Frac	1	0	1	1
Liquid Frac	0	1	0	0

Fig. 28. Worksheet for heat exchanger

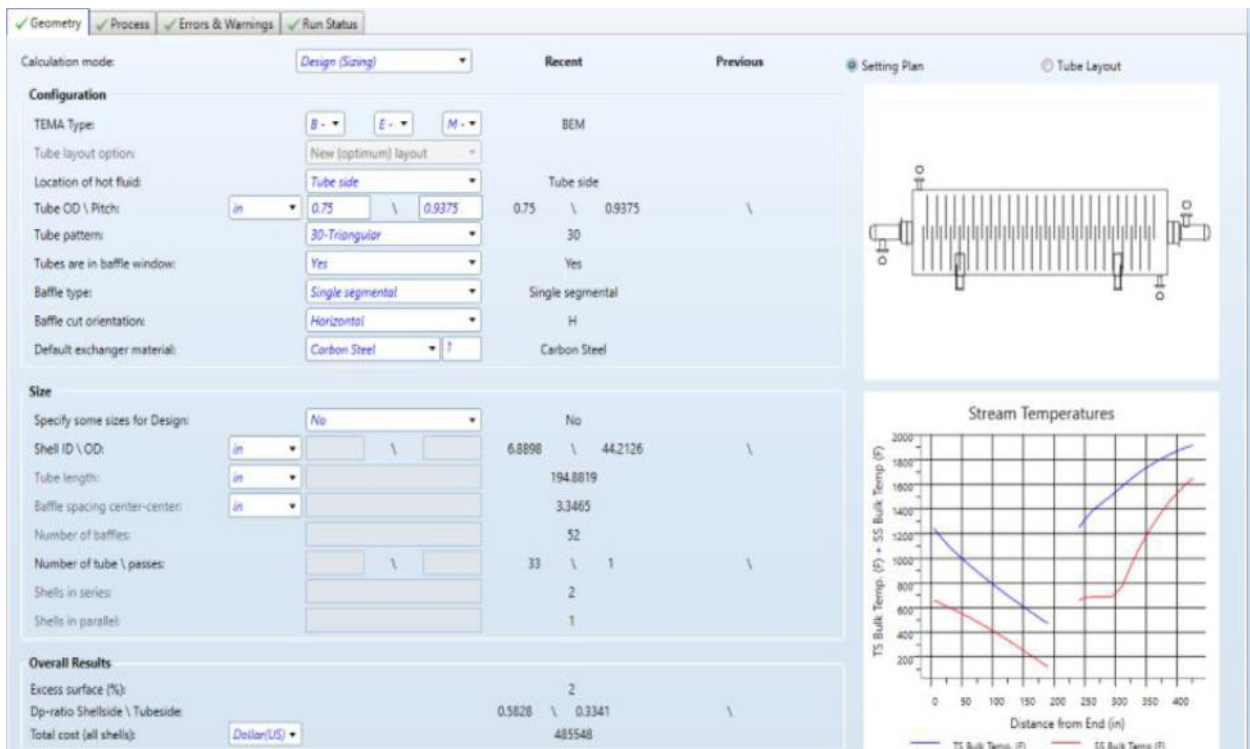


Fig. 29. Exchanger sizing on EDR

3.1 Separator Sizing

The separator sizing is given in Table 4. Feed type is a mixture of ammonia hydrogen and nitrogen are

Table 4
 Separator Sizing

Feed	2036	kmol/h
Flowrates		
NH ₃	899.3	kmol/h
H ₂	852.97	kmol/h
N ₂	284.32	kmol/h
Fractions		
NH ₃	0.441699	
H ₂	0.418944	
N ₂	0.139646	
Liquid	975.3048	kmol/h
Flowrates		
NH ₃	885.535	kmol/h
H ₂	15.9962	kmol/h
N ₂	73.7755	kmol/h
Fractions		
NH ₃	0.907957	
H ₂	0.016401	
N ₂	0.075644	
Vapour	1061	kmol/h
Flowrates		
NH ₃	13.766	kmol/h
H ₂	836.98	kmol/h
N ₂	210.55	kmol/h
Fractions		
NH ₃	0.012975	
H ₂	0.78886	
N ₂	0.198445	
Process Conditions		
T	273.15	K
P	300	bar
T	273.15	K
Molecular weights		
NH ₃	17	g/gmol
H ₂	2	g/gmol
N ₂	28	g/gmol
Densities		
NH ₃	0.6571	g/ml
H ₂	0.022151	g/ml
N ₂	0.3275	g/ml

$MW_l = 17.6151$ g/gmol, $MW_v = 7.36829$ g/gmol and $V_l = 31.43807983$ ml/gmol

Density of Liquid

$$\rho_L = MW_L / V_L \text{ (9)}$$

$$\rho_L = 0.560310938 \text{ g/ml}$$

Density of Vapour; density for ideal gas is

$$\rho_v = PMW_v/RT \quad (10)$$

$$\rho_v = 0.0975938 \text{ g/ml}$$

Mass flowrate of liquid and vapour

$$W_v = 7817.75569 \text{ kg/hr}; W_L = 17180.09158 \text{ kg/hr}$$

Calculation for K

$$F_{LV} = (W_L/W_v) * (\rho_v / \rho_L)^{1/2} \quad (11)$$

$$F_{LV} = 0.917149101 \text{ ft/s}$$

$$K_{drum} = \exp[A + B \ln F_{LV} + C(\ln F_{LV})^2 + D(\ln F_{LV})^3 + E(\ln F_{LV})^4] \quad (12)$$

$$K_{drum} = 0.163913104 \text{ ft/s}$$

Volumetric flowrate of vapours

$$Q_v = W_v / [(3600)(\rho_v)] \quad (13)$$

$$Q_v = 0.785197477 \text{ ft}^3/\text{s}$$

Liquid Volumetric Flowrate

$$Q_L = W_L / [(60)(\rho_L)] \quad (14)$$

$$Q_L = 18.03294486 \text{ ft}^3/\text{min}$$

Terminal Velocity

$$u_{perm} = K_{drum} [(\rho_L - \rho_v) / \rho_v]^{1/2} \quad (15)$$

$$u_{perm} = 0.356911344 \text{ ft/s}$$

$$u_v = 0.267683508 \text{ ft/s}$$

Hold up Volume

$$\text{Hold time} = 0.8 \text{ min}, V_H = 14.42635589 \text{ ft}^3$$

Surge Volume

$$\text{Surge time} = 0.9 \text{ min}, V_s = 16.22965038 \text{ ft}^3$$

Diameter and Total Cross sectional area

$L/D = 5$ (assumed)

$$D = [4 (V_H + V_S) / \lambda (0.6) (L/D)]^{1/3} \quad (16)$$

$D = 2.349874281 \text{ ft} = 2.5 \text{ ft}$

$$A_T = (\lambda/4) D^2 \quad (17)$$

$A = 4.909375 \text{ ft}^2$

Low Level Liquid Height

$H_{LLL} = 9 \text{ inch}$

Low liquid level Area

$H_{LLL}/D = 0.3$

$X = H_{LLL}/D; Y = A_{LLL}/A$

$$Y = (a + cX + eX^2 + gX^3 + iX^4) / (1.0 + bX + dX^2 + fX + X^4) \quad (18)$$

H/D to A/A_T

$Y = A/A_T$

$X = H/D$

$a = 4.755930E-5, b = 3.924091, c = 0.174875, d = -6.358805, e = 5.668973, f = 4.018448, g = -4.91641, h = -1.801705$ and $i = -0.145348$

Figure 30 shows the horizontal two-phase separator.

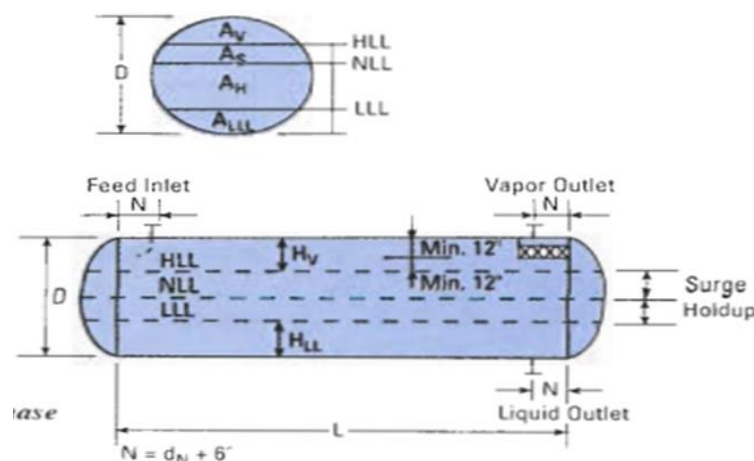


Fig. 30. Horizontal two-phase separator phase

$$Y = 0.152132935$$

$$A_{III} = 0.74687763 \text{ ft}^2$$

Area of Vapor Disengagement

$$H_v = 1 \text{ ft}, X = H_v/D, Y = A_v/A, X = 0.4, Y = 0.206787838$$

$$A_v = 1.01519904 \text{ ft}^2$$

Length to accommodate the liquid and vapor

$$L = (V_{LL} + V_s)/(A_T - A_v - A_{LLL}) \quad (19)$$

$$L = 9.740419576 \text{ ft} = 10 \text{ ft}$$

Liquid drop out time

$$\emptyset = H_v/U_v \quad (20)$$

$$U_{va} = 0.773441902 \text{ ft/s}$$

Minimum length for vapor liquid disengagement

$$L_{min} = U_{VA} \quad (21)$$

$$L_{min} = 2.88938944 \text{ ft}$$

$$L = 10 \text{ ft}$$

Since $L > L_{min}$ so the design is acceptable.

$L \gg L_{min}$ so to reduce the length we need to reduce the value.

H_v which is already at the minimum value so it cannot be further be optimized.

$$L/D = 4 ; \text{ range} = 1.5-6$$

Area of normal liquid level

$$A_{NIL} = A_{LLL} + V_H/L \quad (22)$$

$$A_{NIL} = 2.189513219 \text{ ft}^2$$

3.2 Material and Energy Balance

Figure 31 shows the material balance of the dissociator.

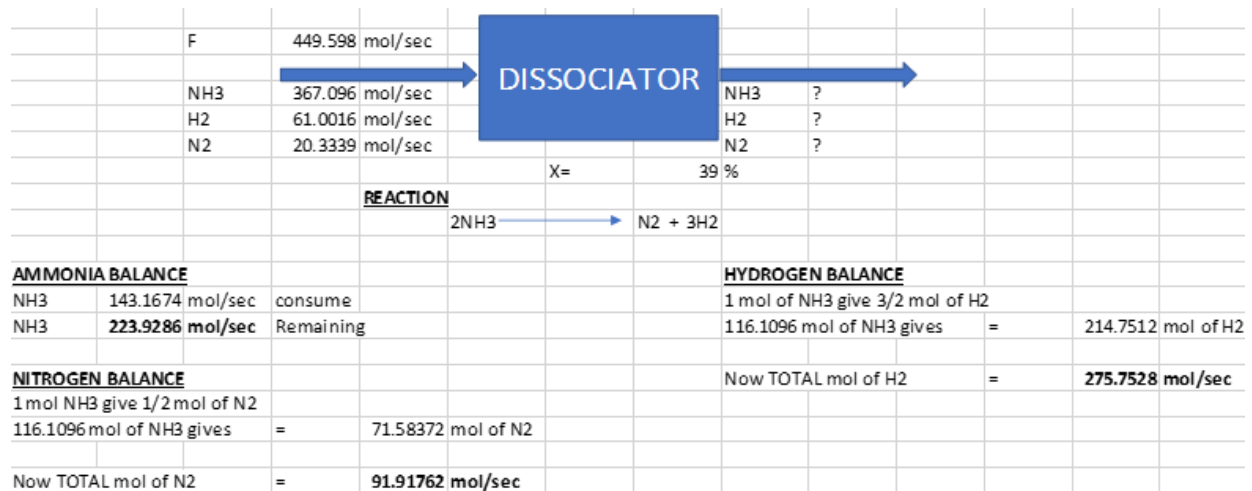


Fig. 31. Material balance of dissociator

Figure 32 shows the material balance of separator.

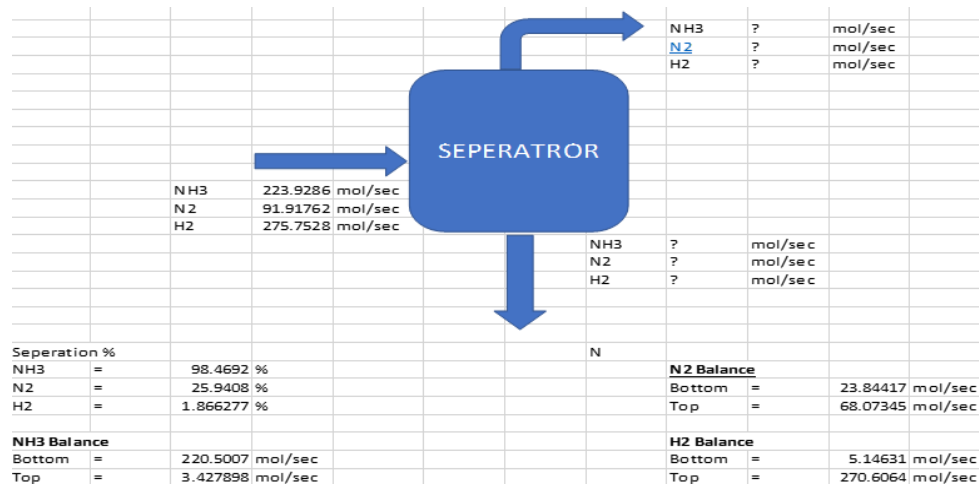


Fig. 32. Material balance of separator

Figure 33 shows the material balance of separator. The reformer unit works at optimum temperature (593 K) and pressure (297.0297 atm) [32, 33].

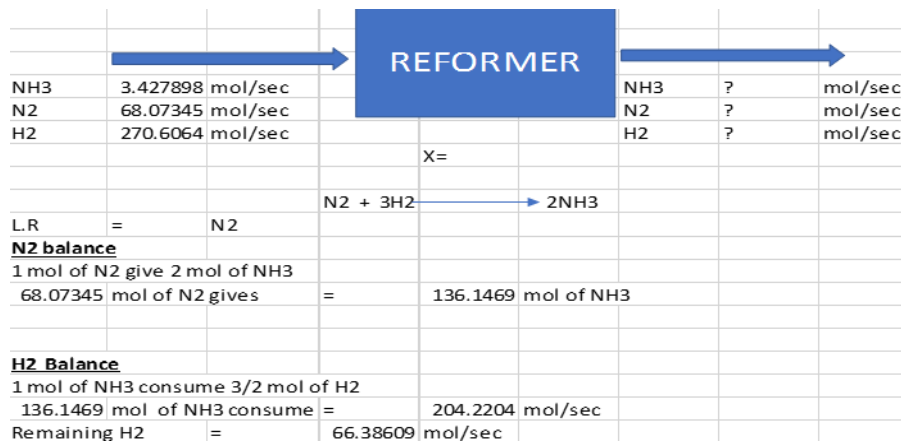


Fig. 33. Material balance of reformer

Figure 34 shows the material balance of the mixer.

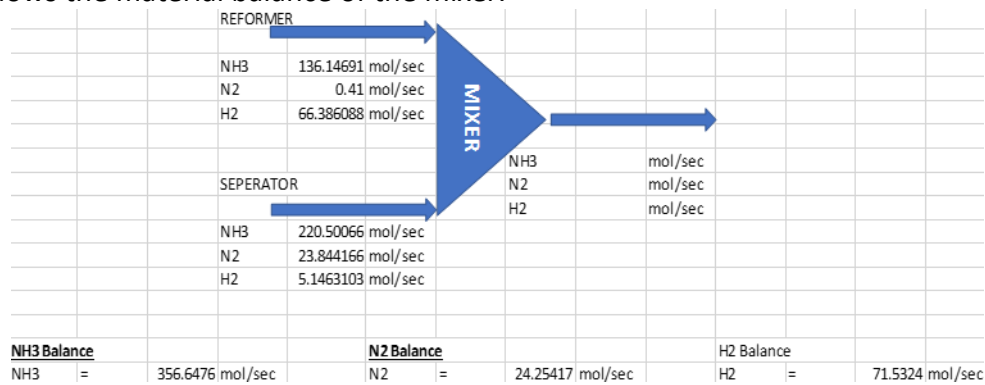


Fig. 34. Material balance of mixer

Figure 35 explains the verification of energy conversion with simulation.

ENERGY REQUIRED TO BREAK THE BOND OF N2 and H2				ENERGY RELEASE FORMING THE BOND			
N2	1 mol required * 225 kcal/mol	=	225	2NH3	2 moles * (3*93 kcal/mol)	=	558
3H2	1 mol required *104 = (3*104) = 312	=	312				Kcal/mol
TOTAL ENERGY ABSORBED		=	537	TOTAL ENERGY RELEASED		=	558 kcal
558 kcal-537 kcal=21 net kcal released for 2 moles of NH3 and 1 mol = 10.5 kcal							
input flowrate			1 mol NH3 =	10.5 Kcal			
NH3	136.6 kmol/sec		1 kcal =	1.16 W h			
Energy Produce		=	5989636.8	5.9896368 MW			
turbine duty		=	2.216165616	MW			

Fig. 35. Verification of energy conversion with simulation

4. Conclusions

From the ammonia-based thermal storage technology, the energy obtained has the least losses as compared to the remaining methods. This method of storing energy makes it possible to run a solar power plant for 24 hrs. This method is environmentally friendly because of the closed looping process and renewable energy production. This method can lead to new horizons of research and development in the field of renewable energy. Proper optimization of this process could lead to satisfactory results in the future. The accomplishment of solar thermal frameworks to generate

electricity hinges very crucially on optimum design selection of an energy storage system that enables the continual operation of the plant. It can be installed in such an area that receives a high intensity of sunlight throughout the whole year. Places like the Thar Desert and interior Sindh in Pakistan are ideal locations for such type of thermal plants.

Acknowledgment

The authors would like to acknowledge the Department of Chemical Engineering and Department of Polymer and Petrochemical Engineering, NED University of Engineering & Technology, Karachi, Pakistan for supporting in this research work.

References

- [1] Zhang, H. L., J. Baeyens, J. Degève, and G. Cacères. "Concentrated solar power plants: Review and design methodology." *Renewable and Sustainable Energy Reviews* 22 (2013): 466-81.
<https://doi.org/10.1016/j.rser.2013.01.032>
- [2] Abghoui, Younes, Anna L. Garden, Jakob G. Howalt, Tejs Vegge, and Egill Skúlason. "Electroreduction of N₂ to Ammonia at Ambient Conditions on Mononitrides of Zr, Nb, Cr, and V: A DFT Guide for Experiments." *ACS Catalysis* 6, no. 2 (2015): 635-46.
<https://doi.org/10.1021/acscatal.5b01918>
- [3] Michalsky, R., A. M. Avram, B. A. Peterson, P. H. Pfromm, and A. A. Peterson. "Chemical looping of metal nitride catalysts: low-pressure ammonia synthesis for energy storage." *The Royal Society of Chemistry* 6 (2015): 3965-74.
<https://doi.org/10.1039/C5SC00789E>
- [4] Cheng, Zhuo, Lang Qin, Jonathan A. Fan, and Liang-Shih Fan. "New Insight into the Development of Oxygen Carrier Materials for Chemical Looping Systems." *Engineering* 4, no. 3 (2018): 343-51.
<https://doi.org/10.1016/j.eng.2018.05.002>
- [5] McEnaney, Joshua M., Aayush R. Singh, Jay A. Schwalbe, Jakob Kibsgaard, John C. Lin, Matteo Cargnello, Thomas F. Jaramillo, and Jens K. Nørskov. "Ammonia synthesis from N₂ and H₂O using a lithium cycling electrification strategy at atmospheric pressure." *The Royal Society of Chemistry* 10 (2017): 1621-30.
<https://doi.org/10.1039/C7EE01126A>
- [6] Shakerian, Farid, Ki-Hyun Kim, Jan E. Szulejko, and Jae-Woo Park. "A comparative review between amines and ammonia as sorptive media for post-combustion CO₂ capture." *Applied Energy* 148 (2015): 10-22.
<https://doi.org/10.1016/j.apenergy.2015.03.026>
- [7] Thengane, Sonal K., Andrew Hoadley, Sankar Bhattacharya, Sagar Mitra, and Santanu Bandyopadhyay. "Thermodynamic evaluation of chemical looping based nitric oxide and hydrogen production." *Chemical Engineering Research and Design* 132 (2018): 252-75.
<https://doi.org/10.1016/j.cherd.2018.01.005>
- [8] Zeng, Liang, Zhuo Cheng, Jonathan A. Fan, Liang-Shih Fan, and Jinlong Gong. "Metal oxide redox chemistry for chemical looping processes." *Nature Reviews Chemistry* 2, no. 11 (2018): 349-64.
<https://doi.org/10.1038/s41570-018-0046-2>
- [9] Luzzi, Andreas, Keith Lovegrove, Ermanno Filippi, Hans Fricker, Manfred Schmitz-Goeb, Mathew Chandapillai, and Stephen Kaneff. "Techno-economic analysis of a 10 MWe solar thermal power plant using ammonia-based thermochemical energy storage." *Solar Energy* 66, no. 2 (1999): 99-101.
[https://doi.org/10.1016/S0038-092X\(98\)00108-X](https://doi.org/10.1016/S0038-092X(98)00108-X)
- [10] Keith, Lovegrove, Andreas Luzzi, Michelle Mccann, and Oliver Freitag. "Exergy analysis of ammonia-based solar thermochemical power systems." *Solar Energy* 66, no. 2 (1999): 103-55.
[https://doi.org/10.1016/S0038-092X\(98\)00132-7](https://doi.org/10.1016/S0038-092X(98)00132-7)
- [11] Johnston, Glen, Keith Lovegrove, and Andreas Luzzi. "Optical performance of spherical reflecting elements for use with paraboloidal dish concentrators." *Solar Energy* 74, no. 2 (2003): 133-40.
[https://doi.org/10.1016/S0038-092X\(03\)00118-X](https://doi.org/10.1016/S0038-092X(03)00118-X)
- [12] Willem, Erisman Jan, Mark A. Sutton, James Galloway, Zbigniew Klimont, and Wilfried Winiwarter. "How a century of ammonia synthesis changed the world." *Nature Geoscience* 1, no. 10 (2008): 636-39.
<https://doi.org/10.1038/ngeo325>
- [13] Dunn Rebecca, Keith Lovegrove, and Greg Burgess. "A review of ammonia-based thermochemical energy storage for concentrating solar power." *Proceedings of the IEEE* 100, no. 2 (2011): 391-400.
<https://doi.org/10.1109/JPROC.2011.2166529>

- [14] Abashar, M. E. E. "Low temperature catalytic reforming of heptane to hydrogen and syngas." *Journal of Saudi Chemical Society* 20 (2016): S186-S95.
<https://doi.org/10.1016/j.jscs.2012.09.019>
- [15] Trevor, Brown. *Round-Trip Efficiency of Ammonia as A Renewable Energy Transportation Media*. Ammonia Energy. Vol. 20, USA: ACS Sustainable Chemistry & Engineering, 2017.
- [16] Wang, Ke, Daniel Smith, and Ying Zheng. "Electron-driven heterogeneous catalytic synthesis of ammonia: Current states and perspective." *Carbon Resources Conversion* 1, no. 1 (2018): 2-31.
<https://doi.org/10.1016/j.crcon.2018.06.004>
- [17] Zhao, Jiankang, Chaonan Cui, Hua Wang, Jinyu Han, Xinli Zhu, and Qingfeng Ge. "Insights into the Mechanism of Ammonia Decomposition on Molybdenum Nitrides Based on DFT Studies." *The Journal of Physical Chemistry C* 123, no. 1 (2018): 554-64.
<https://doi.org/10.1021/acs.jpcc.8b10101>
- [18] Wang, Qianru, Jianping Guo, and Ping Chen. "Recent progress towards mild-condition ammonia synthesis." *Journal of Energy Chemistry* 36 (2019): 25-36.
<https://doi.org/10.1016/j.jechem.2019.01.027>
- [19] Abghoui, Younes, and Egill Skúlason. "Computational Predictions of Catalytic Activity of Zincblende (110) Surfaces of Metal Nitrides for Electrochemical Ammonia Synthesis." *The Journal of Physical Chemistry C* 121, no. 11 (2017): 6141-51.
<https://doi.org/10.1021/acs.jpcc.7b00196>
- [20] Lee, Boreum, Junhyung Park, Hyunjun Lee, Manhee Byun, Chang Won Yoon, and Hankwon Lim. "Assessment of the economic potential: CO-free hydrogen production from renewables via ammonia decomposition for small-sized H₂ refueling stations." *Renewable and Sustainable Energy Reviews* 113 (2019): 109262.
<https://doi.org/10.1016/j.rser.2019.109262>
- [21] Lee, K. M., C. W. Lai, K. S. Ngai, and J. C. Juan. "Recent developments of zinc oxide based photocatalyst in water treatment technology: A review." *Water research* 88 (Jan 1 2016): 428-48.
<https://doi.org/10.1016/j.watres.2015.09.045>
- [22] Heinz, Hendrik, and Hadi Ramezani-Dakhel. "Simulations of inorganic–bioorganic interfaces to discover new materials: insights, comparisons to experiment, challenges, and opportunities." *The Royal Society of Chemistry* 45 (2016): 412-48.
<https://doi.org/10.1039/C5CS00890E>
- [23] Pusara, Srdjan, Simcha Srebnik, and Dario R. Dekel. "Molecular Simulation of Quaternary Ammonium Solutions at Low Hydration Levels." *The Journal of Physical Chemistry C* 122, no. 21 (2018): 11204-13.
<https://doi.org/10.1021/acs.jpcc.8b00752>
- [24] Aziz, Muhammad, Aditya Putranto, Muhammad Kunta Biddinika, and Agung Tri Wijayanta. "Energy-saving combination of N₂ production, NH₃ synthesis, and power generation." *International Journal of Hydrogen Energy* 42, no. 44 (2017): 27174-83.
<https://doi.org/10.1016/j.ijhydene.2017.09.079>
- [25] Aziz, Muhammad, Firman B. Juangsa, Farid Triawan, Asep B.D. Nandiyanto, and Ade G. Abdullah. "Integrated Nitrogen Production and Conversion of Hydrogen to Ammonia." *Chemical Engineering Transactions* 70 (2018): 571-76.
<https://doi.org/10.3303/CET1870096>
- [26] Voitic, G., and V. Hacker. "Recent advancements in chemical looping water splitting for the production of hydrogen." *The Royal Society of Chemistry* 6 (2016): 98267–96.
<https://doi.org/10.1039/C6RA21180A>
- [27] Bao, D., Q. Zhang, F. L. Meng, H. X. Zhong, M. M. Shi, Y. Zhang, J. M. Yan, Q. Jiang, and X. B. Zhang. "Electrochemical Reduction of N₂ under Ambient Conditions for Artificial N₂ Fixation and Renewable Energy Storage Using N₂ /NH₃ Cycle." *Advanced Material* 29, no. 3 (Jan 2017).
<https://doi.org/10.1002/adma.201604799>
- [28] Jiang, Qionqiong, Hao Zhang, Yali Cao, Hui Hong, and Hongguang Jin. "Solar hydrogen production via perovskite-based chemical-looping steam methane reforming." *Energy Conversion and Management* 187 (2019): 523-36.
<https://doi.org/10.1016/j.enconman.2019.01.112>
- [29] Chen, Xiaoyi, Zhen Zhang, Chonggang Qi, Xiang Ling, and Hao Peng. "State of the art on the high-temperature thermochemical energy storage systems." *Energy Conversion and Management* 177 (2018): 792-815.
<https://doi.org/10.1016/j.enconman.2018.10.011>
- [30] Khurana, Maninder, Zhenyuan Yin, and Praveen Linga. "A Review of Clathrate Hydrate Nucleation." *ACS Sustainable Chemistry & Engineering* 5, no. 12 (2017): 11176-203.
<https://doi.org/10.1021/acssuschemeng.7b03238>

-
- [31] More, Amey, Charles J. Hansen, and Götz Vesper. "Production of inherently separated syngas streams via chemical looping methane cracking." *Catalysis Today* 298 (2017): 21-32.
<https://doi.org/10.1016/j.cattod.2017.07.008>
- [32] Balthazar, Pravinth, and Muzathik Abdul Majeed. "Simulation analysis of two-phase heat transfer characteristics in a smooth horizontal ammonia (R717) evaporator tube." *CFD Letters* 10, no. 2 (2018): 49-58.
- [33] Ismail, H., A. A. Aziz, R. A. Rasih, N. Jenal, Z. Michael, and Azmi Roslan. "Performance of Organic Rankine Cycle Using Biomass As Source of Fuel." *Journal of Advanced Research in Applied Sciences and Engineering Technology* 4, no. 1 (2016): 29-46.